5th Asian-Pacific International Symposium on Combustion and Energy Utilization

Flame Holding Performance of Axial Swirlers

W.F. Muniz
Assistant Researcher, INPE, Instituto Nacional de Pesquisas Espaciais, Rod. Presidente Dutra km 40, Cachoeira Paulista, São Paulo, 12630-000, Brazil

H.S. Couto
Senior Researcher, INPE, Instituto Nacional de Pesquisas Espaciais, Rod. Presidente Dutra km 40, Cachoeira Paulista, São Paulo, 12630-000, Brazil

G.L.S. Ribeiro
Laboratory Assistant, INPE, Instituto Nacional de Pesquisas Espaciais, Rod. Presidente Dutra km 40, Cachoeira Paulista, São Paulo, 12630-000, Brazil

D. Bastos-Netto
Senior Researcher, INPE, Instituto Nacional de Pesquisas Espaciais, Rod. Presidente Dutra km 40, Cachoeira
Paulista, São Paulo, 12630-000, Brazil FAX + 55 12 560 9386, E-mail: demetrio@yabae.cptec.inpe.br

The flame holding performance of an axial swirler with continuously variable pitch angle has been analyzed under open, semi-confined and confined conditions. The swirler was assembled around a conventional gas burner, positioned just upstream the quarl and its diameter was smaller than or equal to the secondary air duct. Clear limits were established for the flame anchoring, lifting and blow-out regions as functions of the Swirl Number. The simplicity shown in controlling the flame size and shape suggests greater flexibility to combustion chamber optimization processes. This flame control was confirmed by the use of Image Processing and Treatment techniques.

Keywords: swirlers, flame anchoring, lifting and blowout, image processing.

INTRODUCTION

Swirlers find a lot of use nowadays as flame holders in modern industrial plants and gas turbines in substitution of bluff bodies and screens, as the former ones do not impose large pressure losses to the flow field neither suffer as much as the later from the exposure to elevated temperatures, while still displaying good performance in stabilizing the flame and providing rapid heat release [1, 2]. This wide spread use of swirlers in industry has been the consequence of nearly three decades of intense research in the field of swirling flows, since the early work of Chigier and Beér [3] who first introduced the concept of the swirl number and laid the foundations for the later work [4].

More recently, Weber and Dugué [5] proposed an effective swirl number for well mixed flames to account for the combustion effects on swirl flows and showed that the internal recirculation zone strength could be correlated with that parameter. In their work they achieved an easy control of the swirl level by splitting the inlet air flow into axial and tangential streams and by varying the ratio of the later to the total air flow rate. Movable block swirlers have also been developed and used to the same end, i.e., to achieve an easy control of the swirl level [5 - 7]. As axial swirlers in particular are widely used in industry, this paper describes the flame holding performance of such a device, built with rotating blades in a continuously variable pitch angle, to achieve the desired control of the swirl level.

EXPERIMENTAL SET UP AND PROCEDURE

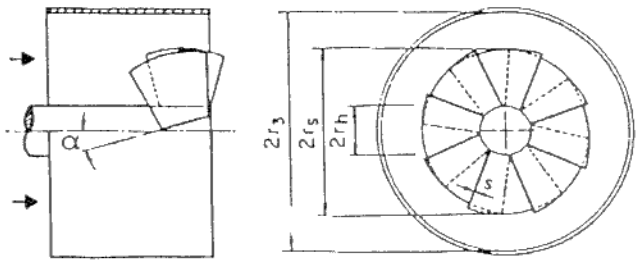

Figure 1 - Axial swirler in an axial flow.
(Taken from reference [8])

Figure 1 shows the sketch of a guide vane swirler in an axial tube flow, where r_h is the hub radius, r_3 is the duct inner radius, r_s is the swirler radius and α is the vane angle. The characteristics of this swirler i.e., the swirl number, S's, the alternative swirl number, S' the permeability, μ, and the blockage coefficient ,C_B, given below, have been calculated in reference [8]:

$$S'_S = \frac{2C_B\left(r_S^3 - r_h^3\right)\tan\alpha}{3\left(r_3 - r_h\right)\left(r_3^2 - r_h^2\right)}, \qquad (1)$$

$$S' = \frac{1}{1+M_R}S'_S, \qquad (2)$$

$$M_R = \frac{\dot{m}_p U_p}{\dot{m}_S U_S} \qquad (3)$$

where $\dot{m}_{p,S}$ and $U_{p,S}$ are the mass flow rates and axial velocities of the primary and secondary flows, respectively,

$$C_B = \left(\frac{1}{1-\sigma}\right) \qquad (4)$$

and

$$\mu = \frac{A_{ef} - A_b}{A_S - A_b} \qquad (5)$$

where

$$\sigma = \left(\frac{A_S - A_{ef}}{A_3 + A_S}\right), \qquad (6)$$

$$A_S = \pi\left(r_S^2 - r_h^2\right), \qquad (7)$$

$$A_S = \pi\left(r_3^2 - r_S^2\right) \qquad (8)$$

and

$$A_{ef} = A_{SS} - A_f + A_b, \qquad (09)$$

with

$$A_{SS} = \pi\left(r_S^2 - r_h^2\right)\cos\alpha, \qquad (10)$$

$$A_f = zs\left(r_S - r_h\right)\cos\alpha \qquad (11)$$

and

$$A_b = z\left(\tan\frac{\pi}{z} - \frac{\pi}{z}\right)r_h^2\sin\alpha, \qquad (12)$$

for a swirler with z vanes of thickness s.

Figure 2 shows the ducted swirler assembled around the fuel injector. Notice the outer ring with interlocking arms which provides an easy and smooth control of the blades pitch angle.

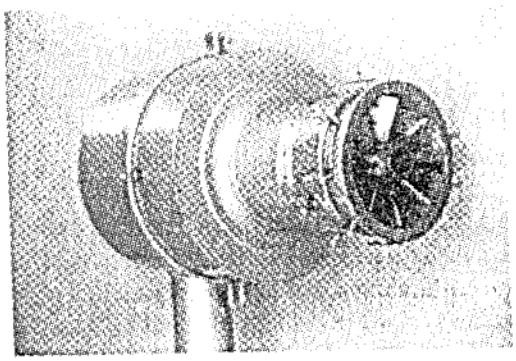

Figure 2 - Ducted swirler

This burner was placed in a test bench and fed with air from a 9 kw fan. The fuel used was LPG which was fed from four 45 kg cylindrical bottles. Four fuel injectors were used in the experiment. They were 250 mm long, 304 stainless steel seamless tubes (with injection holes of 4.0, 5.0, 6.3 and 7.0 mm, each, respectively).

The air and fuel mass flow rates were measured with orifice plates and controlled by flow regulators. Test runs were made under open air, semi-confined (using a 210 mm long, 68° diverging nozzle coupled to the burner exit) and confined conditions.

Pictures were taken during the open air tests for later Image Processing in a Flame Analyzing non Intrusive System (here called SANICH), using 100 ASA Kodak Negative and 100 ASA Daylight Diapositive films and a ratio between the time of exposure and the shutter opening time interval equal to 60/16 was kept in order to obtain clear mean

turbulent flame contours and the flow temperature field. The SANICH system was previously calibrated with pictures taken in the visible and infra-red regions. It employed nine CCD cameras, six of them in the visible and near red wavelength bands and the remaining three in the ultra violet range, 2 PCs with data acquisition cards and specific programs plus a set of filters, each of them operating according to the CCD cameras operational spectra. The SANICH system consists in a Tests Subsystem [TS], an Images Acquisition Subsystem [IAS], a Data Storing Subsystem [DSS], an Images Processing Subsystem [IPS] and a Results Validation Subsystem [RVS], as suggested in the block diagram shown below in Figure 3:

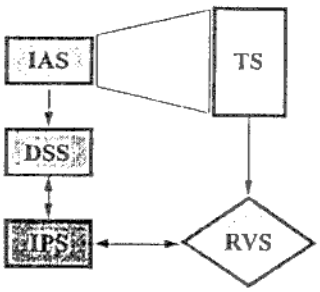

Figure 3: Full SANICH system schematics

Nine runs were made for each one of the fuel injectors, using mass flow rates of 236, 280 and 319 g/s, for conditions of open air, semi-confined and confined flames, in a total of 324 trials.

During each run the swirler blade pitch angle was increased while the secondary air and the fuel mass flow rates were controlled so to establish the flame lifting and blowout regions.

RESULTS

Figures 4 to 6 show S', the alternative swirl number [8] versus Re_p, the Reynolds Number for the fuel injection parameters, i.e.,

$$Re_p = \frac{2\dot{m}_p}{\pi r_i \mu_p} \qquad (13)$$

where μ_p is the fuel dynamic coefficient of viscosity and r_i is the injector radius. The curves fitting were done with the cubic spline technique.

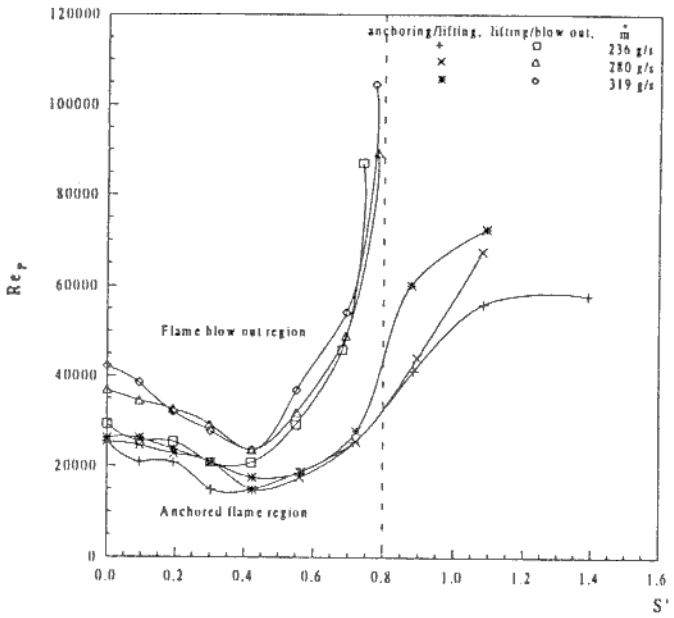

Figure 4 - Open air flame

Figure 4 shows the open air tests results. Notice the well defined regions for flame anchoring and blow-out. The blow-out curves show a common asymptotic value around $S'=0.8$.

The testing under semi-confined and confined conditions, shown in Figures 5 and 6, respectively, still show clearly the flame blow-out boundaries. This is not so, however, with the interface between the flame lifting and anchoring regions, for swirl numbers above 0.42, as shown in those figures. The reason for this was the flame spreading caused by the reduced air entrainment rates plus the quarl visual blocking which precluded a more precise observation of the phenomenon. Notice also that the well known asymptotic value of nearly 0.6 [2, 4] is reached in both cases (actually, $S'=0.62$ and 0.575, for the semi- confined and confined tests, respectively). As expected, the confinement acts to decrease the flame blow-out region as it leads to reduced air entrainment rates and to the blocking effect of the solid boundaries.

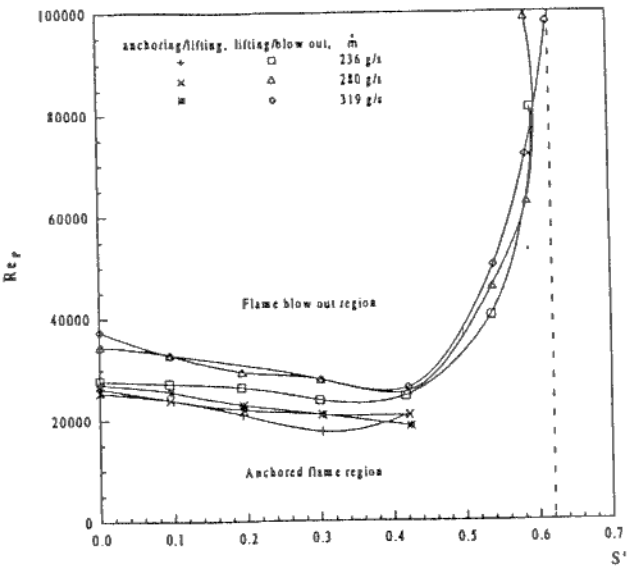

Figure 5 - Semi-confined flame

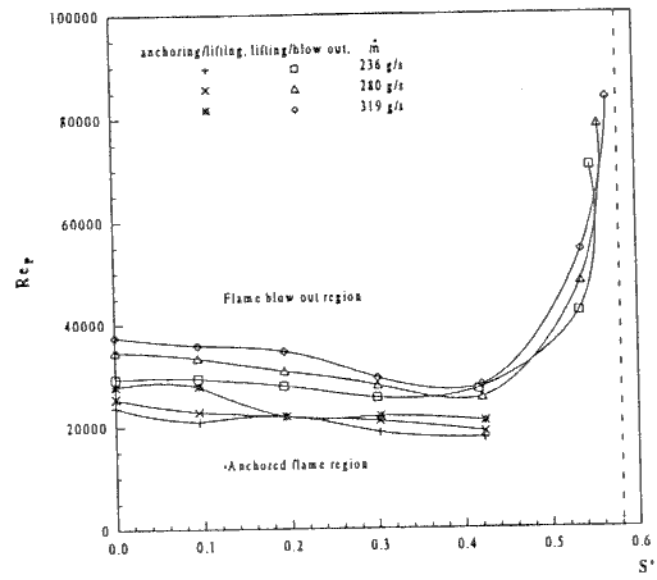

Figure 6 - Confined flame

The picture shown in Figure 7, taken under the conditions described earlier (100 ASA, daylight, diapositive Kodak film) shows an unswirled, anchored, open air flame, fed with 180 g/s of secondary air and 1.30 g/s of fuel (i.e., Re_p=22000).

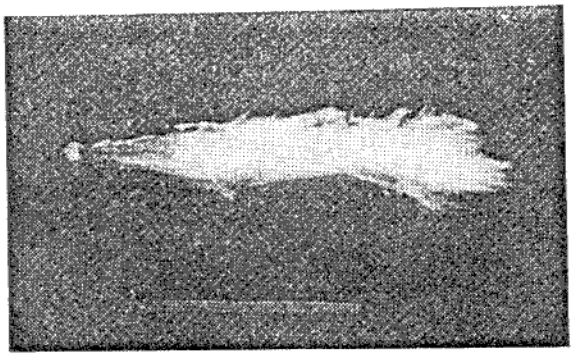

Figure 7 - Open Air Flame - No Swirl

This picture is shown again in Figure 8, after being digitalized in the SANICH Image Processing System. Notice that the different shades show quite clearly the flame surface temperature profile. Actually, regions with the same shade have the same temperature as seen in Figure 8.

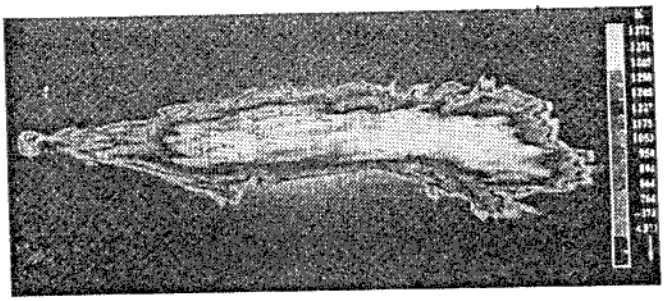

Figure 8 - Digitalized picture of open air flame, no swirl

The increasing of the blades pitch angle to α=40° (S'=1.19), while keeping the flow conditions the same as before, yields the picture shown in Figure 9.

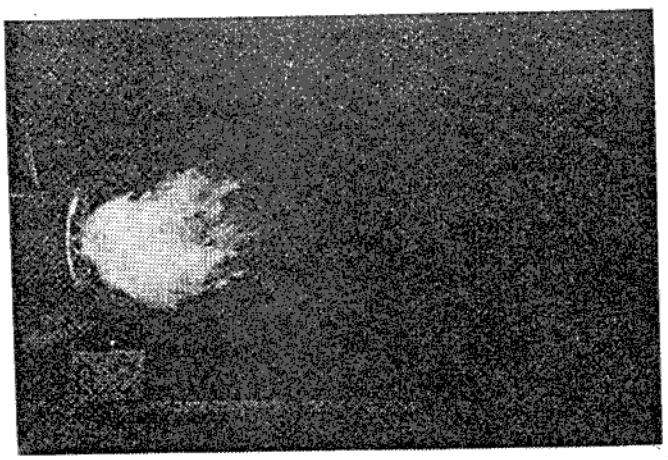

Figure 9 - Open Air Flame - S'=1.190

This open air, anchored, swirled flame picture is showed again in Figure 10 after the above described digitalization process.

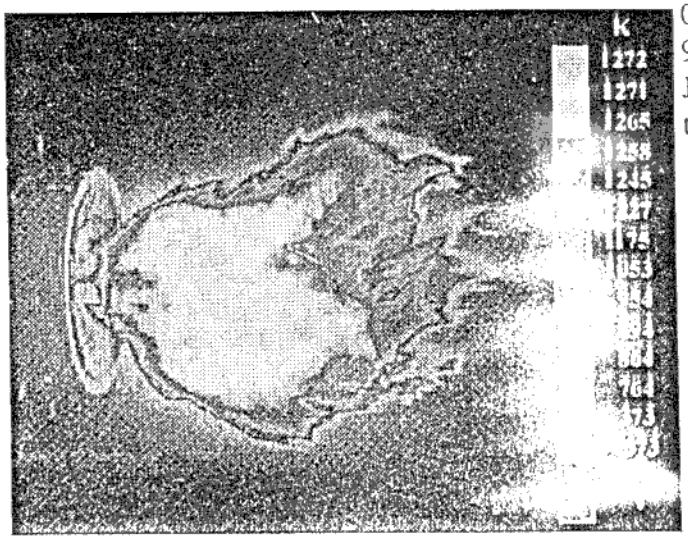

Figure 10 - Digitalized picture of open air flame, S'=1.19

The most external iso-shade region shown in Figure 10 reaches well beyond the flame region, indicating the presence of hot combustion products and the larger, central isothermal region, indicates the presence of an internal recirculation zone (IRZ) and the hot gases expansion process.

Comparison of Figures 7 and 9 show the expected flame widening and shortening caused by the increasing of S', while Figures 8 and 10 suggest that, although the surface temperatures are nearly the same, the flame with the higher swirl number, besides being closer to the injection plane, exhibits a more uniform temperature distribution, due to the existing IRZ. One can say that the IRZ acts as an ignition source for the air/fuel mixture, improving the flame stability.

CONCLUDING REMARKS

Regions for flame blowout, lifting and anchoring conditions in a swirling flow have been established experimentally, using an axial swirler with continuously variable pitch angle assembled around a conventional gas burner, under open air, semi confined and confined conditions. Image digitalization treatment of open-air flame pictures confirmed its usefulness as an excellent tool for flame analysis.

AKNOWLEDGEMENT

This work was done under the sponsorship of CNPq (Contracts Nos. 500140/92-8 and 301406/91-0) and FAPESP (Contracts Nos. 92/1138-8 and 96/10310-0). The authors would like to thank Mr. J.B. Escada and his Image Generation Division for their precious assistance.

NOMENCLATURE

A_{ef} -Effective air passage area across the swirler

A_s - Swirler swept cross-section;

A_3 -Air passage cross-section outside the swirler

C_B -Blockage coefficient;

$\dot{m}_p$, $\dot{m}_s$ -Primary and secondary mass flow rates

Re_p -Reynolds Number for the injection parameters [Eq.(13)];

r_h , r_i , r_3 , r_s -Hub, injector, duct and swirler radii;

S' -Alternative swirl number;

S'_s -Alternative swirl number for secondary flow

s - Vane thickness;

U_p , U_s -Axial velocities, primary and secondary flows;

W- Tangential component, secondary airflow velocity

z - Vanes number;

Greek symbols:

α - Vane angle;

ρ_s - Density of the secondary flow;

ρ_p - Density of the primary flow;

σ - Blockage factor;

μ_p - Fuel dynamic coefficient of viscosity.

REFERENCES

[1] N. Syred, N.A. Chigier and J.M. Beér, "Flame Stabilization in Recirculation Zones of Jets with Swirl", *Thirteenth Symposium (International) on Combustion.* The Combustion Institute, Pittsburgh, Pa., 617-624, (1970).

[2] J.M. Beér and N.A. Chigier, "Combustion Aerodynamics". John Wiley and Sons, New York, (1972).

[3] N.A. Chigier and J.M. Beér, "Velocity and Static Pressure Distributions in Swirling Air Jets Issuing from Annular and Divergent Nozzles". *Journal of Basic Engineering* **86**, 788, 796, (1964).

[4] D.G. Lilley, "Swirl Flows in Combustion: A Review". *AIAA J.* **15**, 8, 1063,1078, (1977).

[5] R.Weber and J. Dugué, "Combustion Accelerated Swirling Flows in High Confinements". *Prog. Energy Combust.* **18**, 349, 367, (1992).

[6] T.F. Wall, "The Combustion of Coal as Pulverized Fuel Through Swirl Burners". Principles of Combustion Engineering for Boilers, Lawn, C. J.(Ed.), Academic Press, New York, N.Y., 197-335, (1987).

[7] M.P. Heap, T.M. Lowes and R. Walmsley, "Emission of Nitric Oxide from Large Turbulent Diffusion Flames". *Fourteenth Symposium (International) on Combustion.* The Combustion Institute, Pittsburgh, Pa., 885-895 (1973).

[8] H.S. Couto, , W.F. Muniz and D.Bastos-Netto, "Geometrical Parameters for Flows across Axial Swirlers", *Proceedings of The Third Asian-Pacific International Symposium on Combustion and Energy Utilization*, Hong Kong, 11-15 December, 1995, Vol. I, pp. 255-260, (1995)